

Particle Physics Catalysis of Thermal Big Bang Nucleosynthesis

Maxim Pospelov^{1,2}

¹*Perimeter Institute for Theoretical Physics, Waterloo, Ontario N2J 2W9, Canada*

²*Department of Physics and Astronomy, University of Victoria, Victoria, British Columbia, V8P 1A1 Canada*

(Received 1 July 2006; revised manuscript received 9 November 2006; published 4 June 2007)

We point out that the existence of metastable, $\tau > 10^3$ s, negatively charged electroweak-scale particles (X^-) alters the predictions for lithium and other primordial elemental abundances for $A > 4$ via the formation of bound states with nuclei during big bang nucleosynthesis. In particular, we show that the bound states of X^- with helium, formed at temperatures of about $T = 10^8$ K, lead to the catalytic enhancement of ${}^6\text{Li}$ production, which is 8 orders of magnitude more efficient than the standard channel. In particle physics models where subsequent decay of X^- does not lead to large nonthermal big bang nucleosynthesis effects, this directly translates to the level of sensitivity to the number density of long-lived X^- particles ($\tau > 10^5$ s) relative to entropy of $n_{X^-}/s \lesssim 3 \times 10^{-17}$, which is one of the most stringent probes of electroweak scale remnants known to date.

DOI: 10.1103/PhysRevLett.98.231301

PACS numbers: 26.35.+c, 14.80.Ly, 98.80.Ft

Standard big bang nucleosynthesis (SBBN) is a well-established theory that makes predictions for elemental abundances of light elements, H, D, He, and Li, as functions of only one free parameter, the ratio of baryon to photon number densities. Agreement of the observed abundances for D and ${}^4\text{He}$ with the SBBN predictions that use an additional cosmic microwave background (CMB)-derived [1] input value of $n_b/s = 0.9 \times 10^{-10}$ serves as a sensitive probe of new physics. Indeed, over the years a finessed SBBN approach has led to constraints on several nonstandard scenarios, including constraints on the total number of thermally excited relativistic degrees of freedom [2]. This first class of constraints results essentially from the distortion of the time frame for the n/p freeze-out, affecting mostly the abundance of ${}^4\text{He}$. The second class of constraints comes from the nonthermal big bang nucleosynthesis (BBN), that results from the late decay of metastable heavy particles [3]. If such decays happen during or after BBN, they trigger electromagnetic cascades that affect light elements via photodissociation, or lead to nonthermal nuclear reactions by fast hadrons produced in the decay, resulting in significant modifications of D, ${}^6\text{Li}$, ${}^7\text{Li}$, and ${}^3\text{He}/\text{D}$ abundances. The BBN constraints have been instrumental in limiting some variants of supersymmetric (SUSY) models with long-lived unstable particles. For example, late decays put constraints on the energy density of unstable gravitinos, limiting it to be less than $\sim 10^{-13}$ relative to entropy $\times \text{GeV}$ [4–6] for some selected range of lifetimes and standard model (SM) branching ratios. It is important to establish whether the late decay of heavy particles can possibly “cure” [4–6] what is known as the lithium problem, a statistically significant and persistent discrepancy of the SBBN prediction for ${}^7\text{Li}$ from the roughly twice smaller observational value over a wide range of metallicities.

The purpose of this Letter is to show that, in addition to the change of the timing for BBN reaction and nonthermal processes, there is a third way particle physics can signifi-

cantly affect the prediction for primordial abundances of light elements. This new way consists of the *catalysis* of thermal nuclear reactions by heavy relic particles that have long-range (electromagnetic or strong) interactions with nuclei. In particular, we show that the cosmological presence of metastable charged particles, called X^- hereafter, enables the catalyzed BBN (CBBN) via the formation of bound states between light nuclei and negatively charged particles X^- . These bound states form in the range of temperatures from 1 to 30 keV, changing the standard nuclear reaction rates but more importantly opening new channels for thermal reactions and changing the abundance of Li and other elements with $A > 4$. The most significant difference is seen in the ${}^6\text{Li}$ production mechanism,

$$\text{SBBN: } {}^4\text{He} + \text{D} \rightarrow {}^6\text{Li} + \gamma; \quad Q = 1.47 \text{ MeV}, \quad (1)$$

$$\text{CBBN: } ({}^4\text{He}X^-) + \text{D} \rightarrow {}^6\text{Li} + X^-; \quad Q \approx 1.13 \text{ MeV}, \quad (2)$$

and, as we are going to show, the cross section for the CBBN channel is enhanced by 8 orders of magnitude relative to SBBN. In (2) and below, (NX) denotes the bound state of a nucleus N and X^- . In the remainder of this Letter, after a brief review of the relevant bound states (NX) , we analyze the cross section and thermal rate for reaction (2), make a prediction for ${}^6\text{Li}$ in CBBN, put constraints on some of the particle physics scenarios, and point out new CBBN mechanisms for ${}^7\text{Li}$ depletion.

Properties of the bound states.—Here we assume that the electromagnetic force is acting between nuclei and X^- particles, and calculate properties of the ground states using the variational approach. Binding energies E_b , average distances between the center of the nucleus and X^- , and the “photodissociation decoupling” temperatures T_0 , are summarized in Table I where the constraint $m_{X^-} \gg m_N$ is also imposed. The main uncertainty in Table I comes from the charge distribution inside the nucleus as the naive

TABLE I. Properties of the bound states: Bohr a_0 and nuclear radii R_N in femtometers; binding energies E_b and “photodissociation decoupling” temperatures T_0 in kilo-electron-volts.

Bound state	$ E_b^0 $	a_0	R_N^{sc}	$ E_b(R_N^{\text{sc}}) $	R_{Nc}	$ E_b(R_{Nc}) $	T_0
$^4\text{HeX}^-$	397	3.63	1.94	352	2.16	346	8.2
$^3\text{HeX}^-$	299	4.81	1.76	276	2.50	267	6.3
$^7\text{LiX}^-$	1566	1.38	2.33	990	3.09	870	21
$^7\text{BeX}^-$	2787	1.03	2.33	1540	3	1350	32
$^8\text{BeX}^-$	3178	0.91	2.44	1600	3	1430	34
TX^-	75	9.6	2.27	73	2.27	73	1.8
DX^-	50	14	...	49	2.75	49	1.2
pX^-	25	29	...	25	1.10	25	0.6

Bohr orbit $a_0 = (Z\alpha m_N)^{-1}$ can be well within the nuclear radius. It leads to a reduction of the bound state energies relative to the Bohr-like formula, $E_b^0 = Z^2\alpha^2 m_N/2$ from $\sim 13\%$ in (^4HeX) to 50% in (^8BeX). Realistic binding energies are calculated for two types of nuclear radii assuming a uniform charge distribution: for the simplest scaling formula $R_N^{\text{sc}} = 1.22A^{1/3}$, and for the nuclear radius determined via the root mean square charge radius, $R_{Nc} = (5/3)^{1/3}R_c$ with experimental input for R_c where available. Finally, as an indication of the temperature at which (NX) are no longer ionized, we include a scale T_0 where the photodissociation rate $\Gamma_{\text{ph}}(T)$ becomes smaller than the Hubble rate, $\Gamma_{\text{ph}}(T_0) = H(T_0)$. It is remarkable that stable bound states of (^8BeX) exist, opening up a path to synthesize heavier elements such as carbon, which is not produced in SBBN. In addition to atomic states, there exist molecular bound states (NXX). The binding energy of such molecules relative to (NX) is not small [e.g., about 300 keV for ($^4\text{HeX}^-X^-$)]. Such neutral molecules, along with (^8BeX) and ($^8\text{BeXX}$), are an important path for the synthesis of heavier elements in CBBN. One can easily generalize Table I for the case of doubly charged particles, which was recently discussed in [7] in connection with the dark matter problem.

The initial abundance of X^- particles relative to baryons, $Y_X(t \ll \tau) \equiv n_{X^-}/n_b$, along with their lifetime τ are the input parameters of CBBN, and it is safe to assume that $Y_X \ll 1$. The most important catalytic enhancement results from the bound states (^4HeX). Their abundance relative to the total abundance of X^- , $Y_{\text{BS}} = n_{\text{BS}}/n_{X^-}$ is calculated using the Boltzmann equation

$$-HT \frac{dY_{\text{BS}}}{dT} = \langle \sigma_{\text{rec}} v \rangle (1 - Y_{\text{BS}}) n_{\text{He}} - \langle \sigma_{\text{ph}} v \rangle Y_{\text{BS}} n_{\gamma} \quad (3)$$

along with the photoionization and recombination cross section. The result is shown in Fig. 1, where a significant deviation from the naive Saha equation is observed as the recombination rate of X^- and ^4He is only marginally larger than the Hubble rate. For the same reason the abundance of bound states with rare light elements is very low, $n_{NX^-}/n_{X^-} \lesssim 10^{-6}$, where $N = ^3\text{He}$, D, and T. As we are

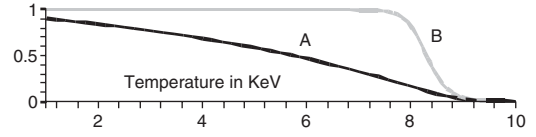


FIG. 1. Fraction of X^- locked in the bound state with ^4He : (A) Realistic result based on Boltzmann equation, (B) Saha-type prediction with a rapid switch from 0 to 1 at $T \approx 8.3$ keV.

going to show, an actual abundance of X^- at $T \approx 8$ keV has to be less than 10^{-6} , which makes the overall impact of these bound states on BBN negligible.

Photonless production of ^6Li .—The standard mechanism for ^6Li production in SBBN is “accidentally” suppressed. The D- ^4He cluster description gives a good approximation to this process, and the reaction rate of (1) is dominated by the E2 amplitude because the E1 amplitude nearly vanishes due to an (almost) identical charge-to-mass ratio for D and ^4He . In the E2 transition, the quadrupole moment of D- ^4He interacts with the gradient of the external electromagnetic field, $V_{\text{int}} = Q_{ij}\nabla_i E_j$. Consequently, the cross section at BBN energies scales as the inverse fifth power of photon wavelength $\lambda = \omega^{-1} \sim 130$ fm, which is significantly larger than the nuclear distances that saturate the matrix element of Q_{ij} , leading to strong suppression of (1) relative to other BBN cross sections [8]. For the CBBN process (2), the real photon in the final state is replaced by a virtual photon, Fig. 2, with a characteristic wavelength on the order of the Bohr radius in ($^4\text{HeX}^-$). Correspondingly, one expects the enhancement factor in the ratio of CBBN to SBBN cross sections to scale as $(a_0\omega)^{-5} \sim 5 \times 10^7$. Figure 1 presents a schematic depiction of both processes. It is helpful that in the limit of $R_N \ll a_0$ we can apply factorization, calculate the effective $\nabla_i E_j$ created by X^- , and relate SBBN and CBBN cross sections *without* explicitly calculating the $\langle \text{D}^4\text{He} | Q_{ij} | ^6\text{Li} \rangle$ matrix element. A straightforward quantum-mechanical calculation with $\nabla_i E_j$ averaged over the hydrogenlike initial state of (^4HeX) and the plane wave of ^6Li in the final state leads to the following relation between the astrophysical S factors at low energy:

$$S_{\text{CBBN}} = S_{\text{SBBN}} \frac{8}{3\pi^2} \frac{p_f a_0}{(\omega a_0)^5} \left(1 + \frac{m_{\text{D}}}{m_{^4\text{He}}}\right)^2. \quad (4)$$

Here a_0 is the Bohr radius of ($^4\text{HeX}^-$), $p_f = [2m_{^6\text{Li}}(Q_{\text{CBBN}} + E)]^{1/2}$ is the momentum of the outgoing ^6Li in the CBBN reaction, and ω is the photon energy in the SBBN process, $\omega = Q_{\text{SBBN}} + E$. For $E \ll Q$ the value of the final momentum of the ^6Li nucleus is

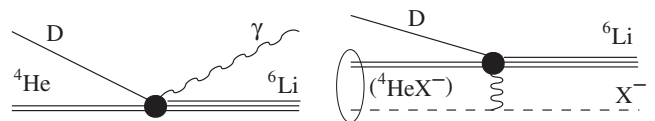


FIG. 2. SBBN and CBBN mechanisms for producing ^6Li .

$p_f \simeq (1.8 \text{ fm})^{-1}$. Throughout the whole Letter, $c = \hbar = 1$. The S factor is defined in the standard way, by removing the Gamow factor G from the cross section: $S(E) = E\sigma/G$. A somewhat more sophisticated approach with the use of an optimized wave function for (${}^4\text{He}X$) in the initial state and the Coulomb wave function in the final state, with the radial integrals calculated with the constraint $|\mathbf{r}_X - \mathbf{r}_{{}^6\text{Li}}| > 2 \text{ fm}$, renders the result, which is very close to a naive estimate:

$$S_{\text{CBBN}}(0) \simeq (6 \times 10^7) \frac{S_{\text{SBBN}}(E_0)}{(1 + E_0/Q_{\text{SBBN}})^5} \simeq 0.3 \text{ MeVb}. \quad (5)$$

Here the SBBN value of $S_{\text{SBBN}} = 1.8 \times 10^{-2} \text{ eVb}$ is taken at some matching scale $E_0 = 0.41 \text{ MeV}$ [9], which is sufficiently close to 0, yet is in the regime where SBBN cross sections can be reliably measured. The result of the factorized approach (5) should be within a factor of a few from the exact answer, with the largest errors presumably associated with the R_N/a_0 expansion. Using the Gamow energy that accounts for the charge screening in (${}^4\text{He}X^-$) and the change of the reduced mass,

$$E_{\text{SBBN}}^{\text{Gamow}} = 5249 \text{ keV} \rightarrow E_{\text{CBBN}}^{\text{Gamow}} = 1973 \text{ keV}, \quad (6)$$

we calculate the thermally averaged cross section for the CBBN processes at small temperatures $T \sim 10 \text{ keV}$ employing a saddle point approximation:

$$\begin{aligned} \langle \sigma_{\text{C}v} \rangle &\simeq 2 \text{ b} \times T^{-2/3} \exp(-23.7T^{-1/3}) \\ &= (1.8 \times 10^9) T_9^{-2/3} \exp(-5.37T_9^{-1/3}). \end{aligned} \quad (7)$$

In the second line, the cross section is converted to customary units of $N_A^{-1} \text{ cm}^3 \text{ s}^{-1} \text{ mole}^{-1}$, and T_9 is temperature in units of 10^9 K . CBBN rate (7) is to be compared with the SBBN expression [8],

$$\langle \sigma_{\text{S}v} \rangle \simeq 30 T_9^{-2/3} \exp(-7.435 T_9^{-1/3}), \quad (8)$$

and the enhancement of 8 orders of magnitude for CBBN is traced back directly to (5). Although tremendously enhanced relative to (8), the CBBN rate (7) is by no means larger than the usual photonless reaction rates known to SBBN.

Catalytic enhancement of ${}^6\text{Li}$ at $6 \lesssim T \lesssim 12 \text{ keV}$.— Armed with the rate (7), we write down the evolution equation for ${}^6\text{Li}$ abundance at $T \lesssim 12 \text{ keV}$:

$$-HT \frac{d{}^6\text{Li}}{dT} = D(n_{\text{BS}} \langle \sigma_{\text{C}v} \rangle + n_{\text{He}} \langle \sigma_{\text{S}v} \rangle) - {}^6\text{Li} n_p \langle \sigma_p v \rangle. \quad (9)$$

In this formula, D and ${}^6\text{Li}$ are the hydrogen-normalized abundances of these elements, n_p and H are the temperature-dependent concentration of free protons and the Hubble rate, and $\langle \sigma_p v \rangle$ is the rate for ${}^6\text{Li} + p \rightarrow {}^3\text{He} + {}^4\text{He}$ responsible for the destruction of ${}^6\text{Li}$ [8]. We use the output of the SBBN code for D , ${}^4\text{He}$ as function of T and solve the CBBN subset of Eqs. (3) and (9) numerically. In fact, since $n_{\text{BS}}(T)$ significantly differs from zero only below 9 keV, the variation of ${}^4\text{He}$ and D abundances is

negligibly small compared to the freeze-out values ($D = 2.4 \times 10^{-5}$, $Y_p = 0.25$). Several of the numerical solutions to this equation for different input values of Y_X and τ are plotted in Fig. 3. The increase in time of ${}^6\text{Li}$ below 10 keV is a direct consequence of CBBN. One can clearly see that with $Y_X \sim O(0.01)$ one could convert up to a few percent of D to ${}^6\text{Li}$. Taking the limit of large lifetime ($\tau > 10^5 \text{ s}$), and using the limiting abundance of primordial ${}^6\text{Li}$ of 2×10^{-11} [4], we get a remarkable sensitivity to X^- :

$$Y_X \lesssim 3 \times 10^{-7} \rightarrow n_{X^-}/s \lesssim 2.5 \times 10^{-17}. \quad (10)$$

A scan over the lifetime parameter produces the exclusion boundary on the $(\tau, \log_{10} Y_X)$ plane plotted in Fig. 4. Also shown is the natural range for Y_X calculated using the standard freeze-out formula with the input annihilation cross section in the range of $\sigma_{\text{ann}} v = (1-100) 2\pi \alpha^2 m_X^{-2}$ and $m_X = 0.1-1 \text{ TeV}$. Taken literally, the ${}^6\text{Li}$ overproduction constrains the heavy charged particles to the range of lifetimes

$$\tau \lesssim 5 \times 10^3 \text{ s}, \quad (11)$$

unless $\sigma_{\text{ann}} v$ is tuned to larger values. In fact, both results, (10) and (11), should be interpreted as limits of sensitivity to (τ, Y_X) via the CBBN enhancement. It is true that excessive energy injection at later time may reduce the amount of ${}^6\text{Li}$ generated in CBBN, and as a consequence relax the constraints of Eq. (10) [10]. The combined analysis of two effects, the CBBN enhancement of ${}^6\text{Li}$ and impact of energy release on elemental abundances, has to be done by combining the result of this work and previous papers on unstable particles in BBN [4–6]. However, such analysis is necessarily model dependent, and falls outside the scope of the present Letter. In many models, however, the decay of X^- is not involving huge energy release, and then both (10) and (11) hold unconditionally.

CBBN points towards an intriguing possibility for alleviating the lithium problem. As is evident from Fig. 3, lifetimes of X^- between 2000 and 5000 s can create a primordial source for ${}^6\text{Li}$ thus removing some tension between observations of ${}^6\text{Li}$ in low metallicity systems and explanation of its production using cosmic rays

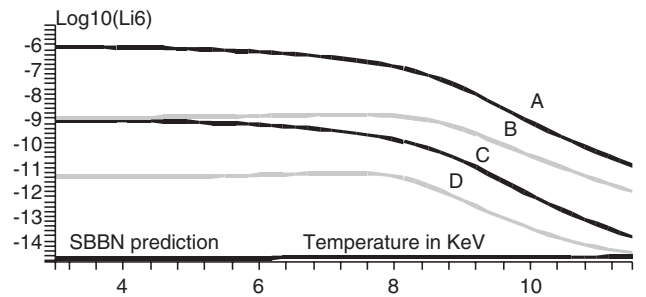


FIG. 3. $\log_{10}({}^6\text{Li})$ plotted as a function of T in kilo-electronvolts for different choices of τ and Y_X : (A) $\tau = \infty$ and $Y_X = 10^{-2}$, (B) $\tau = 4 \times 10^3 \text{ s}$ and $Y_X = 10^{-2}$, (C) $\tau = \infty$ and $Y_X = 10^{-5}$, (D) $\tau = 4 \times 10^3 \text{ s}$ and $Y_X = 10^{-5}$.

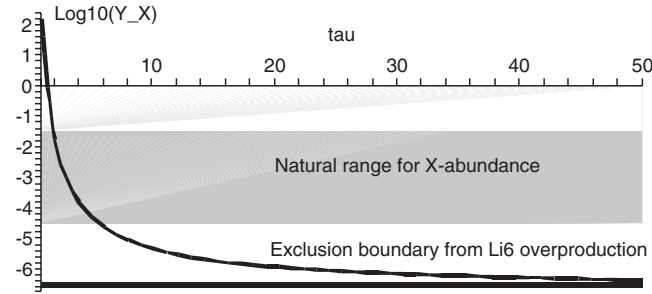


FIG. 4. Constraint on initial abundance of X^- . $\log_{10}(Y_X)$ is plotted against τ in units of 10^3 s. The thick horizontal line is the asymptotic exclusion boundary (10).

[6,11]. But more importantly, such lifetimes of X^- can lead to an overall reduction of ${}^7\text{Li}$ abundance. At the CMB-determined baryon density, most of ${}^7\text{Li}$ is produced via ${}^7\text{Be}$. At $T \sim 30$ keV and $\tau \sim (2-5) \times 10^3$ s X^- is still present in sufficient quantities to trigger the formation of $({}^7\text{Be}X^-)$. Once formed, $({}^7\text{Be}X^-)$ facilitates several reaction rates that destroy ${}^7\text{Be}$. The decay of X^- within the bound state leads to further depletion of ${}^7\text{Be}$ and ultimately of ${}^7\text{Li}$. Moreover, if the decay of X^- occurs via a virtual W boson, there exists a fast electroweak capture process of X^- on ${}^7\text{Be}$, which also leads to an overall depletion of ${}^7\text{Li}$.

Usually, a serious obstacle on the way to solve the Li problem is the abundance of D and ${}^3\text{He}/\text{D}$ ratio [4–6] affected through large energy release, but we emphasize that CBBN mechanism itself is inconsequential for lighter elements such as D or ${}^3\text{He}$ as the abundance of *any* bound states of X^- relative to baryons is not larger than 10^{-6} once the ${}^6\text{Li}$ bounds are satisfied.

Particle physics applications.—There are two generic possibilities for a long-lived X^- : either the decay of X^- is suppressed by tiny couplings, or it decays to another neutral relic state X^0 with small energy release. Schematically, these possibilities can be represented by

$$\begin{aligned} \text{type I: } X^- &\rightarrow \text{SM}^-[X^0], & \Delta E &\sim M_X, \\ \text{type II: } X^- &\rightarrow X^0 + e^-[\nu], & \Delta E &\lesssim \text{few MeV}, \end{aligned} \quad (12)$$

where the first type corresponds to a decay into charged SM state(s) with or without any neutral non-SM relics, and the second type is X^- decaying to another neutral relic plus an electron and possibly some neutrino states with a small energy release. SUSY models have scenarios of both types. An example of type I is the charged slepton (e.g., stau) decaying into gravitinos or decaying due to R -parity violation without leaving any SUSY remnants. Since the amount of energy released in the decay of X^- of type I is large, we cannot restrict this scenario only to the CBBN-enhanced output of ${}^6\text{Li}$ as nonthermal BBN may provide equally important changes in the elemental abundance. In the case of very late decays the constraints coming from, e.g., diffuse γ -ray and microwave backgrounds can become important.

Prior to this work, models of type II were believed to be of no consequence for BBN. Type II models are not involving significant energy release, and therefore our results based on CBBN enhancement, Eqs. (10) and (11), become strict limits rather than levels of sensitivity. Examples of type II include an important case of near-degenerate states of lightest and next-to-lightest SUSY particles, neutralino-chargino or stau-neutralino. Using recent calculation (Ref. [12]) of stau lifetime, we can translate (11) into the limit on *minimal* mass splitting in the stau-neutralino system, $m_{\tilde{\tau}} - m_{\chi} > 70$ MeV. Along the same lines, one can derive constraints on the minimal mass splitting between neutral and charged particles at the first excited Kaluza-Klein level in models with “universal” extra dimensions.

To conclude, thermal catalysis of BBN reactions represents the novel idea of how particle physics can alter the predictions for light elemental abundances. The catalysis of ${}^6\text{Li}$ via the production of $({}^4\text{He}X^-)$ bound states is explicitly demonstrated, and the enormous enhancement in the catalyzed channel furnishes the sensitivity to X^- normalized on entropy at the 3×10^{-17} level.

I would like to thank C. Bird and K. Koopmans for assistance in some calculations and useful discussions and acknowledge useful conversations with Dr. R. Allahverdi, Dr. R. Cyburt, Dr. K. Olive, Dr. A. Ritz, and Dr. Y. Santoso.

-
- [1] D. N. Spergel *et al.* (WMAP Collaboration), *Astrophys. J. Suppl. Ser.* **148**, 175 (2003).
 - [2] For a review of BBN constraints see, e.g., S. Sarkar, *Rep. Prog. Phys.* **59**, 1493 (1996).
 - [3] D. Lindley, *Astrophys. J.* **294**, 1 (1985); J. R. Ellis, D. V. Nanopoulos, and S. Sarkar, *Nucl. Phys.* **B259**, 175 (1985); R. J. Scherrer and M. S. Turner, *Phys. Rev. D* **33**, 1585 (1986); M. H. Reno and D. Seckel, *Phys. Rev. D* **37**, 3441 (1988); S. Dimopoulos *et al.*, *Nucl. Phys.* **B311**, 699 (1989).
 - [4] R. H. Cyburt, J. R. Ellis, B. D. Fields, and K. A. Olive, *Phys. Rev. D* **67**, 103521 (2003).
 - [5] M. Kawasaki, K. Kohri, and T. Moroi, *Phys. Rev. D* **71**, 083502 (2005); K. Jedamzik, arXiv:hep-ph/0604251;
 - [6] K. Jedamzik, *Phys. Rev. D* **70**, 063524 (2004); K. Jedamzik *et al.*, arXiv:hep-ph/0512044; see also M. Kusakabe, T. Kajino, and G. J. Mathews, *Phys. Rev. D* **74**, 023526 (2006).
 - [7] K. M. Belotsky, M. Y. Khlopov, and K. I. Shibaev, arXiv:astro-ph/0604518, and references therein.
 - [8] L. Kawano, Fermilab Report No. FERMILAB-PUB-88-034-A.
 - [9] J. Kiener *et al.*, *Phys. Rev. C* **44**, 2195 (1991).
 - [10] M. Kaplinghat and A. Rajaraman, *Phys. Rev. D* **74**, 103004 (2006).
 - [11] E. Rollinde, E. Vangioni-Flam, and K. A. Olive, *Astrophys. J.* **627**, 666 (2005).
 - [12] T. Jittoh *et al.*, *Phys. Rev. D* **73**, 055009 (2006).